Emergent Materials
https://doi.org/10.1007/s42247-024-00843-6

ORIGINAL ARTICLE

# Polysaccharide polyelectrolyte complex for hydrophobic drug loading and controlled release

**Jindrayani Nyoo Putro[1,2] · Hana Fransisca Tulus[3] · Christian Julius Wijaya[2,3] · Dave Mangindaan[4,5] · Wenny Irawaty[3] · Chintya Gunarto[3] · Nathania Puspitasari[3] · Artik Elisa Angkawijaya[6] · Astrid Rahmawati[7] · Osamu Shimomura[7] · Suryadi Ismadji[2,3]**

Received: 27 June 2024 / Accepted: 14 August 2024


## Abstract

The use of natural-based polymer is currently limited due to its hydrophilic properties. This study investigates durian seed gum for applying a drug delivery system with the combination of chitosan as complex coacervate. The successful synthesis of durian seed gum–chitosan polyelectrolyte complex (PEC) occurred through the electrostatic interaction between gum and chitosan, confirmed by the FTIR spectra and $H^1$ NMR of PEC. The analysis of Zeta Potential also showed the behavior of pH-responsive material, 3.42 mV in pH 2.0 and − 28.8 in pH 7.4. Other characterizations, such as SEM, TGA, DSC, and particle size analysis, were conducted to understand PEC's characteristics further. The entrapment efficiency of dexamethasone using PEC was greater than 90%, with a high loading content of around 4 mg/gram PEC. The drug release profile from PEC follows the mechanism of polymer swelling and non-Fickian diffusion. The combination of durian seed gum and chitosan as a coacervate greatly enhances the controlled release of hydrophobic drugs. This suggests that durian seed gum–chitosan PEC has promising potential for use in pharmacokinetic research.

**Keywords** Polyelectrolyte complex · Durian seed gum · Chitosan · pH-responsive · Dexamethasone release

## 1 Introduction

Gum is a complex heteropolysaccharide with more than one type of monosaccharide in its structure; it is also considered a biodegradable and biocompatible material, which makes it suitable for use as a drug excipient in the pharmaceutical industry or as a controlled release media for biostimulants and antimicrobial agents for agrochemical applications [1, 2]. Because of their nature as rheological modifiers, several seed gums (guar gum, basil seed gum, durian seed gum, and tamarind seed gum) have been extensively studied by researchers for various applications, such as emulsifiers, stabilizers, and ingredient improvement, in the food industry [3–6]. Indonesia is an agricultural country with a tropical climate, so various kinds of fruit and agricultural products can thrive. One of the most well-known agricultural products is durian, which produced around 1.13 million tons in 2020 [7]. Durian fruit (*D. zibethinus Murr*) consists of fruit, shell, and seed; only 1/3 of the durian can be consumed. The shell and seed are discarded after consumption as solid waste; seeds contribute about 20–25% of the total fruit weight.

✉ Jindrayani Nyoo Putro
jindrayani@ukwms.ac.id

1 Chemical Engineering Master Program, Faculty of Engineering, Widya Mandala Surabaya Catholic University, Kalijudan 37, Surabaya 60114, Indonesia

2 Collaborative Research Center for Sustainable and Zero Waste Industries, Jl. Kalijudan 37, Surabaya, East Java 60114, Indonesia

3 Department of Chemical Engineering, Widya Mandala Surabaya Catholic University, Kalijudan 37, Surabaya 60114, Indonesia

4 Professional Engineer Program Department, Faculty of Engineering, Bina Nusantara University, K.H. Syahdan No. 9, Jakarta 11480, Indonesia

5 Waste-Food-Environmental Nexus Research Interest Group, Bina Nusantara University, K.H. Syahdan No. 9, Jakarta 11480, Indonesia

6 Plant Lipid Research Team, RIKEN Center for Sustainable Resource Science, Yokohama 230- 0045, Japan

7 Department of Applied Chemistry, Osaka Institute of Technology, 5-16-1 Omiya, Ashahi-ku, Osaka 535-8585, Japan

Published online: 05 September 2024

Durian seed gum mainly consists of monosaccharides, fatty acids, protein, and prebiotics [8–10]. Most studies have focused on extraction methods and other applications in the food industry, such as emulsifiers in mayonnaise and encapsulating agents for probiotic bacteria [5, 11]. No study has utilized gum from durian seeds for application in oral drug delivery systems. The limitation of using natural polymers like durian seed gum is the hydrophilic nature since the major functional groups in the material are hydroxyl groups. Apart from that, there are several advantages to utilizing durian seed gum as a drug carrier, including its competitive economic value compared with commercially available gum (e.g., xanthan gum, alginate, or guar gum), lack of competition with the food supply chain, nutraceutical value, and low glycemic index, which are beneficial for individuals with type II diabetes mellitus [12]. Considering these values, durian seed gum is a promising feedstock in the drug delivery system. However, a modification of durian seed gum is needed to overcome the limitation of its hydrophilicity. The combination of gum-chitosan has been studied as a drug carrier in various drug delivery systems, which was known as polyelectrolyte complex (PEC).

PEC or complex coacervates have been extensively studied in the pharmaceutical industry as coating materials, dissolution rate enhancers, and binding agents in drug formulations [13]. PEC is formed by dropping a polyanion solution on a chitosan solution or vice versa, generally leading to the system dissociation of ionic groups or electrostatic interactions. Chitosan is widely used in drug delivery because of its natural origin and biocompatibility; for example, the combination of various types of gum and chitosan PEC has been investigated as a carrier for triamcinolone [14], metformin hydrochlorite [15], ofloxacin [16–18], secnidazole [19], curcumin [20], ibuprofen [21], tamoxifen citrate [22], and naproxen [23].

Li et al. investigated various anionic polysaccharides, such as carboxymethyl cellulose, sodium alginate, carrageenan, and xanthan gum, with chitosan as a complex coacervate for the release of theophylline and metoprolol succinate. Their results showed that the amount of theophylline released from the xanthan gum–chitosan coacervate was slower than that released from other anionic polysaccharides (up to 50% cumulative release within 10 h) [24]. The slightly soluble drug (theophylline) is more strongly associated with the xanthan gum–chitosan complex. Minkal et al. (2018) studied the hydrophobic drug ofloxacin, which was entrapped using carboxymethyl gum katira–chitosan for controlled drug release. The cumulative release of ofloxacin was maintained at 20% for 2 h at pH 2.0, and the sustained release reached 84% within 24 h at pH 6.8. Combining anionic and cationic polysaccharide PEC is a promising approach for controlled hydrophobic drug release.

Dexamethasone (DEX) is a synthetic corticosteroid compound used as a multipurpose drug for its anti-inflammatory and immune suppressive effects. It is used for acute COVID-19 patients, reducing the mortality rate of patients requiring oxygen or ventilator support [25, 26]. Several studies have investigated the controlled release of hydrophobic DEX using β-cyclodextrin, montmorillonite-polylactic-co-glycolic acid, poly(ethylene glycol) methyl ether – poly(lactic acid) – acryloyl chloride hydrogel, polyvinyl alcohol hydrogel, and hybrid hydrogel [27–31]. These methods use complex steps of material synthesis compared to PEC. It is also one of the most effective micro/nanoencapsulation methods in the food and pharmaceutical industries [32]. Polysaccharide complex coacervate is nontoxic, well-tolerated, and biocompatible compared to chemical synthetic materials, which often involve toxic or hazardous chemicals in their synthesis [33].

This research aimed to extract gum from durian seeds and analyze the application of durian seed gum to deliver hydrophobic drugs using PEC. Using a simple coacervate complex procedure, this study entrapped DEX among anionic and cationic polysaccharides. The optimum conditions for the separation of gum from durian seeds were investigated. This gum was further utilized as a microparticle coacervate with chitosan as the carrier of hydrophobic DEX. The effect of the durian seed gum and chitosan ratio was examined to determine the highest production yield of the microparticles. Afterward, drug incorporation and release experiments were performed to understand better the influence of the durian seed gum-chitosan complex coacervate.

## 2 Materials and methods

### 2.1 Materials

Tapanuli durian seed (*Durio zibethinus* Murr.) was obtained from Pargarutan, South Tapanuli district, North Sumatera province, Indonesia. Low molecular weight (MW) chitosan (Sigma Aldrich, Lot BCCD9854) with a degree of acetylation ≥ 75% and a viscosity of 20–300 cps in 1% wt. of acetic acid solution (concentration of 1% wt.) was used as one of the raw materials for PEC synthesis. Dexamethasone (Sigma Aldrich, D4902, ≥ 98% HPLC), ethanol (Merck, Lot I1153783, ACS spectrophotometric grade > 95%), glacial acetic acid (Merck, Lot K53509263, ≥ 99%), HCl (Honeywell Fluka, Lot H2400, ACS reagent, ≥ 37%), NaOH (Supelco, Lot MB2032798, ACS reagent, ≥ 97%), NaCl (Merck, Lot K45005604, ACS reagent, ≥ 99%), KCl (Merck, Lot K51302936, ACS reagent, 99.0-100.5%), $KH_2PO_4$ (Supelco, Lot AM1605873, ACS reagent, ≥ 99%), and $Na_2HPO_4$ (Sigma Aldrich, Lot SLCK8884, ACS

**Table 1** Setting levels of the aqueous extract of durian seed gum

| Parameters | Range | | Outside Range | | Units |
|---|---|---|---|---|---|
| | Low | High | -1 | +1 | |
| Time | 20 | 40 | 10 | 50 | min |
| W: S* | 30:1 | 50:1 | 20:1 | 60:1 | w/w |
| pH | 11 | 13 | 10 | 14 | - |
| Temperature | 60 | 80 | 50 | 90 | °C |

*W: S indicates the ratio of water to durian seed

reagent, ≥ 99%) were used without further purification. Deionized water was used throughout this study.

## 2.2 Methods

### 2.2.1 Extraction of gum from durian seed

The durian seeds were rinsed thoroughly with deionized water to remove dirt and dust and then partially dried using a heating oven at 60 °C to reduce the moisture content. The hull and embryo of the dried durian seed were removed, leaving only the endosperm. The endosperm was ground and passed through an 80-mesh sieve to obtain a homogeneous particle size of around 170 µm. The durian seed powder was then stored and sealed in a dry place for further use.

Durian seed powder was extracted using an aqueous solution under different conditions [8]. The parameters used for this extraction were time, water: seed ratio (W: S), pH, and temperature, as shown in Table 1. For pH adjustment, 0.1 M NaOH was used to control the pH of the aqueous extract. These various conditions involved 54 sets of extraction conditions in duplicate; these parameter sets were based on the statistical model of central composite design (CCD) using product yield as the determinant. The seed-water slurry was stirred using a heating mantle with a condenser to minimize water loss. The slurry was centrifuged at 1200 rpm for 10 min to collect the supernatant. The supernatant was mixed with 95% ethanol three times to separate the precipitate. The precipitate was collected and oven-dried at 60 °C. All the experiments were performed using deionized water. The yield of durian seed gum was determined using Eq. (1).

$$Y = \frac{M_1}{M_2} \times 100 \tag{1}$$

where $Y$ represents the extraction yield (%), $M_1$ is the mass of extracted gum (g), and $M_2$ is the initial mass of the durian seed (g). The masses of the extracted gum and durian seeds were both dry.

Response surface methodology (RSM) was used to predict the effect of four variables of gum extraction ($x_1$ as extraction time, $x_2$ as water-to-seed ratio, $x_3$ as aqueous pH, and $x_4$ as extraction temperature) on the extraction yield (%) of durian seed gum. These experimental data are then processed using a central composite design (CCD) with one central point and six-star points to obtain points outside the range (-1 and +1) with the possibility of unexpected response changes that may occur outside that range. The response function (Y), which is the extraction yield, was generalized with a second-order polynomial model to predict the variation in the response variables given below:

$$Y = b_0 + b_1x_1 + b_2x_2 + b_3x_3 + b_4x_4 + b_{11}x_1^2 + b_{22}x_2^2 + b_{33}x_3^2 + b_{44}x_4^2 + b_{12}\times_1 x_2 + b_{13}\times_1 x_3 + b_{14}\times_1 x_4 + b_{23}\times_2 \times_3 + b_{24}\times_2 x_4 + b_{34}\times_3 x_4$$

This model was represented by $b_0$ as a constant coefficient; $b_1$, $b_2$, $b_3$, and $b_4$ as linear coefficients; $b_{11}$, $b_{22}$, $b_{33}$, and $b_{44}$ as quadratic coefficients; and $b_{12}$, $b_{13}$, $b_{14}$, $b_{23}$, $b_{24}$, and $b_{34}$ as interaction coefficients, as shown in Table 2. $R^2$ and adjusted $R^2$ represented the adequacy of the model.

**Table 2** Regression coefficients of aqueous extraction variables

| Source | | Regression Coefficient |
|---|---|---|
| **Model** | $b_0$ | 13.72 |
| Main Effects | $b_1$ | 0.26 |
| | $b_2$ | -0.52 |
| | $b_3$ | 16.28 |
| | $b_4$ | -3.62 |
| Quadratic Effects | $b_{11}$ | 0.27 |
| | $b_{22}$ | 0.65 |
| | $b_{33}$ | 5.63 |
| | $b_{44}$ | 1.17 |
| Interaction Effects | $b_{12}$ | -1.25 |
| | $b_{13}$ | -0.008 |
| | $b_{14}$ | 0.98 |
| | $b_{23}$ | -0.29 |
| | $b_{24}$ | -2.75 |
| | $b_{34}$ | -6.77 |
| **$R^2$** | | 0.94 |
| **Adjusted-$R^2$** | | 0.92 |

*Significant at $p < 0.05$; $b_0$, $b_1$, $b_2$, $b_3$, and $b_4$ represent the intercept, main effect of time, W:S ratio, pH, and temperature, respectively. $b_{11}$, $b_{22}$, $b_{33}$, and $b_{44}$ represent the quadratic effects of time, W:S ratio, pH, and temperature, respectively. $b_{12}$, $b_{13}$, $b_{14}$, $b_{23}$, $b_{24}$, and $b_{34}$ represent the interaction effects of time and W: S ratio, time and pH, time and temperature, W:S ratio and pH, W:S ratio and temperature, and between pH and temperature, respectively

### 2.2.2 Preparation of DEX dispersion in the gum solution

A total of 0.5 g of gum was dissolved in 100 mL sodium hydroxide solution (pH 13.2). The gum was stirred for 2 h at 70 °C. DEX was dissolved in ethanol at a predetermined concentration. The DEX solution was further dispersed into a gum solution that was cooled before adding DEX. The dispersion of DEX solution in gum is called DEX@

gum, which was mixed until a homogeneous dispersion was obtained.

#### 2.2.3 Preparation of complex coacervate chitosan and DEX@gum

The DEX@gum solution was slowly added to the chitosan and prepared in advance. Two grams of 100 mL of chitosan was dissolved in 2% acetic acid solution (pH 3.9). The coacervate was subsequently centrifuged for 30 min at 4,900 rpm. The supernatant was collected to measure unloaded DEX in the aqueous system, while the solid was kept at -20 °C and freeze-dried. The entrapment of DEX in PEC was labeled DEX@PEC, and the amount of DEX entrapped in the PEC was measured using a UV–Vis spectrophotometer at a wavelength of 240 nm. The amount of entrapped drug and the entrapment efficiency were calculated using Eqs. (2) and (3), respectively. Blank PEC was prepared using a similar method without the addition of DEX.

$$LC = \frac{(DEX_{initial} - DEX_{final})V}{m} \tag{2}$$

$$EE = \frac{DEX_{\text{initial}} - DEX_{\text{final}}}{DEX_{\text{initial}}} \times 100 \tag{3}$$

where $LC$ is the loading content (mg/g), $EE$ is the entrapment efficiency (%), $V$ is the volume of solution (L), $m$ is the mass of PEC (g), and $DEX_{initial}$ and $DEX_{final}$ are defined as the initial and final concentrations of DEX (mg/L), respectively.

#### 2.2.4 Kinetic release of DEX@PEC

An in vitro drug release study of DEX@PEC was conducted in simulated gastric and intestinal fluid. First, 0.5 g of DEX@PEC was immersed in 500 mL of simulated gastric fluid (SGF) with a pH of 2.0; SGF was prepared by dissolving NaCl and HCl without pepsin. Simultaneously, 0.5 g of DEX@PEC was added to 500 mL of simulated intestinal fluid (SIF) prepared using 10 mM phosphate-buffered saline (PBS) (pH 7.4). The solution was then heated to 37 °C and stirred at 100 rpm. At the specified time, 2 mL of the solution was removed, and 2 mL of the new medium was added to the system. The release of free drugs was also studied by dissolving DEX in ethanol and placing it in SGF and SIF due to the limited solubility of DEX in aqueous media. Before analysis with a UV/Vis spectrophotometer at a wavelength of 240 nm, the sample was first separated between the solution and the solid by centrifugation. The release profile was calculated using the following equation:

$$\text{Release profile } (\%) = \frac{M_t}{M_o} \times 100 \tag{4}$$

where $M_t$ and $M_o$ are the released and initial drug-loaded concentrations in the PEC, respectively, and the release profile was plotted as a function of the concentration versus time.

#### 2.2.5 Swelling studies

The PEC blanks' swelling degree (SD) was determined simultaneously in SGF and SIF solutions at 37 °C. This test was conducted to determine the swelling ability of PEC blanks at pH 2.0 (SGF) and pH 7.4 (SIF) for 48 h. The swelling experiment was carried out in duplicate, and the degree of swelling was calculated using Eq. (5). The swollen and dried PEC masses are Ms (g) and Md (g).

$$SD(\%) = \frac{M_s - M_d}{M_d} \times 100 \tag{5}$$

#### 2.2.6 Analysis of the sugar content of durian seed gum

250 mg of durian seed gum was hydrolyzed in 50 mL of 1 M $H_2SO_4$ at 80 °C for 24 h. Hydrolyzed gum was placed under a rotary evaporator for 4 h at 40 °C under vacuum, and then 25 mL of deionized water was added to the solution and passed through a nylon membrane filter of 0.22 µm for further analysis. The sugar composition was determined using a high-performance liquid chromatography (HPLC: Shimadzu LC-2030 C 3D) instrument equipped with a refractive index (RI) detector and an oven. Sulfuric acid (5 mM) was used as the mobile phase with a flow rate of 0.6 mL/min and a temperature of 80 °C. The analytical column was a Coregel 87H3 (ID 7.8 mm × length 300 mm, particle size 9 µm).

#### 2.2.7 Characterization of DSG and Chitosan complex coacervates

**2.2.7.1** FTIR The FTIR spectrum of each sample was obtained using an FTIR Bruker Tensor II instrument equipped with an ATR platinum accessory; the KBR pellet method was used, and measurements were carried out in the wavenumber range of 4000–500 $cm^{-1}$.

**2.2.7.2** $^1$H nuclear magnetic resonance (NMR) The sample of PEC and durian seed gum were dissolved in $CDCl_3$. The solution was prepared by dissolving 20 mg of the sample in 0.5 mL $CDCl_3$ with tetramethylsilane (TMS) as an internal

standard; it was mixed at 80 °C for 6 h. The mixture was cooled down and examined by $^{1}H$ NMR. The spectra were recorded on a JEOL ECZ400s spectrometer (JEOL, Tokyo, Japan) at 400 MHz. The monosaccharides of glucose and galactose were also measured to check the sugar backbone of the PEC.

**2.2.7.3** SEM The material morphology was analyzed using scanning electron microscopy (SEM JEOL JIB-4610 F) with an emission gun at 10 kV. The samples were coated with gold (Au) for 90 s before SEM analysis.

**2.2.7.4** Zeta potential and particle size analysis The zeta potential and particle size were determined by a ZetaSizer Nano ZS90 (Malvern Panalytical); the samples were prepared in a solution with a concentration of 1% wt and measured using the dynamic light scattering technique.

**2.2.7.5** Differential scanning calorimetry Differential scanning calorimetry (DSC) measurements were performed using a Perkin Elmer DSC 8000 instrument under an inert gas ($N_2$) flow rate of 20 mL/min with a constant heating rate of 10 °C/min.

**2.2.7.6** Thermal gravimetry analysis Thermal gravimetric analysis (TGA) was performed on a LINSEIS L70/2171 thermistor under $N_2$ atmosphere conditions at temperatures ranging from 30 °C to 600 °C using a heating rate of 10 °C/min.

## 3 Results and discussions

### 3.1 Statistical analysis of the extracted DSG

The correlation between the four extraction variables and the extraction yields as a response function was carried out using response surface analysis. Table S1 (refer to the supplementary data) shows the matrix design of the yield data obtained from the four variables. Figure S1 shows the plot of the predicted vs. actual yield of gum obtained in this study, a linear regression with an $R^2$ of 0.97. Figure S1 shows that two data sets had negative values. However, the distribution of the data yield is satisfactory to the regression line, which shows no significant differences between the predicted and experimental yields.

RSM analysis can determine the influencing variables and interactions between variables that occur during the extraction of durian seed gum. The regression coefficients obtained can be seen in Table 2. A high $^{R2\ value}$ indicates that the model can represent the experimental data. However, a high $R^2$ did not mean the regression model was good. The adjusted $R^2$ could be used to evaluate the differences between $R^2$ and adjusted $R^2$. Table 2 shows that $R^2$ and adjusted $R^2$ did not differ significantly, implying that the model did not include significant terms [34]. The interaction effects of aqueous extraction variables with high $R^2$ values indicate a good fit model with a value of 0.94 (minimum of 0.80). However, the response of the extraction results obtained from the regression coefficient data is negatively related to the ratio of water to solid and pH. Conversely, the extraction time or temperature is positively proportional to the linear and quadratic effects.

Thus, the response surface to represent this interaction is shown in Fig. 1(a-f). The interaction between pH and other variables shows that the extraction yield increases with increasing pH and time ($b_{13}$); this is the opposite of the increase in the W: S and temperature ($b_{23}$) variables, which decrease the yield.

As shown in Fig. 1, the temperature of this extraction process significantly influenced the yield. A more concentrated alkaline solution provides a more elevated extraction yield, which agrees with the observation reported by [35, 36]. Therefore, extraction at high pH should be chosen for higher yields. As shown in the data under the extraction condition of pH 11, the low yield occurs due to the inability of low alkaline conditions to hydrolyze the mucus in the endosperm. Interestingly, Table S1 shows that at pH 10, no gum was found in the extraction. This phenomenon explains why a high pH is necessary for gum extraction, as excess hydroxide ions are needed to attack the glycosidic bonds in polysaccharides [37].

In the durian seed extraction process, temperature has the opposite effect compared to pH. Increasing the extraction temperature decreased the yield due to the hydrolysis of polysaccharides at high temperatures [38]. Thus, as shown in Fig. 1(a), the interaction effect of pH was more significant than the temperature effect, with the optimum effect occurring at pH 13 and 60 °C.

The interaction between pH and W: S (Fig. 1(b)) shows that excess water results in greater extraction yields at high alkalinity. Excess water is the driving force causing more liquid-binding water-soluble components in the endosperm to diffuse out of the seed. This condition results in less sticky extraction, thus increasing the extraction yield of the mucilage. In conclusion, excessive water was chosen to obtain a high extraction yield, which in this work was 50:1 (Fig. 1b) [39, 40].

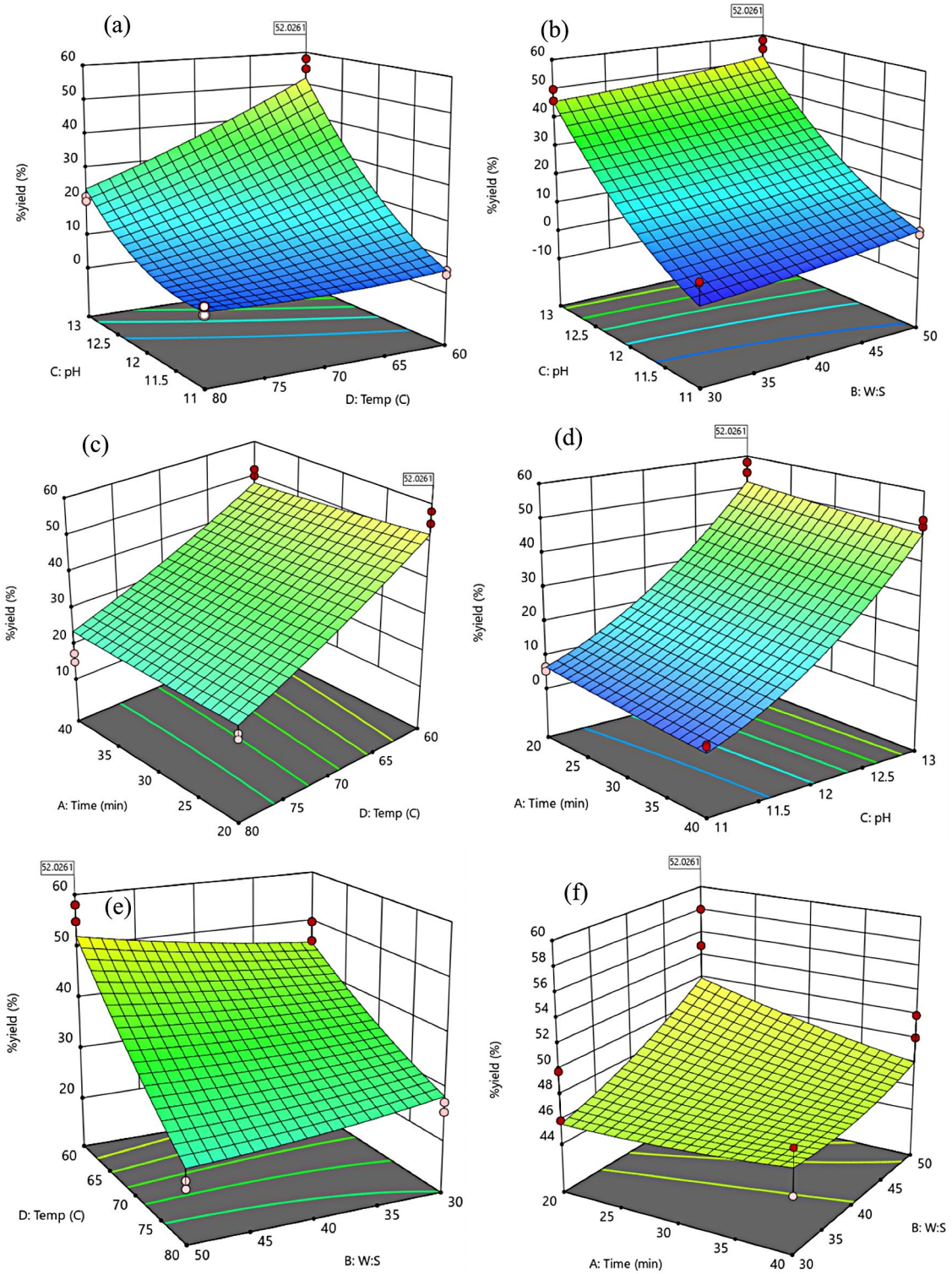


**Fig. 1** Response surface of aqueous extraction variables in extraction yield against (**a**) pH and temperature for 20 min and W: S = 50; (**b**) pH and W: S for 20 min at 60 °C; (**c**) Temperature and Time at pH 13 and W: S = 50; (**d**) Time and pH for W: S = 50 at 60 °C; (**e**) Temperature and W: S at pH 13 for 20 min; and (**f**) Time and W: S at pH 13 at 60 °C

The extraction time did not significantly affect the increase in yield (Fig. 1(c)). The results show a slight increase in extraction results in a short time; at long extraction times, the results tend to be constant. Increasing the extraction time will change the polysaccharide structure [40]. Figure 1(c) indicates that the time effect is the least significant variable for this model. The optimum extraction time to produce gum with the highest yield was 20 min. The optimum conditions for extracting gum from durian seeds were 20 min, a pH of 13, a temperature of 60 °C, a water-to-solid ratio of 50:1, and a yield of 58%. This result was greater than that of Amin et al., who reported that crude durian seed gum yield was 18% [41]. A similar yield of durian seed gum (56.4%) was reported by [39]; however, the set of variables differed. A previous study reported that the optimum parameters were W/S = 35.5:1, a temperature of 85 °C, a pH of ~ 12, and an extraction time of 1 h. This study showed a significantly shorter extraction time and relatively lower temperature than the reported study.

## 3.2 Sugar composition of durian seed gum (DSG)

A dilute alkaline solution was used to extract the gum from the durian seeds. Durian seed gum has a monosaccharide sugar profile of 38% glucose, 4.88% galactose, and 1.4% arabinose (Run 15, the highest yield); the original durian seed flour has a sugar composition of 52% glucose, 5.1% galactose, and 0.94% arabinose. As reported in a previous study, the monosaccharide profile revealed that durian seed gum is not a galactomannan. The glucose percentage is similar to that reported by Amid et al. (2012) (around 40%); however, this study produced a low content of galactose (a previous study had a 58% composition of galactose) and a higher content of arabinose than a previous study (0.6%) [9]. Based on this study and previous research, it can be confirmed that durian seed gum is not galactomannan (no mannose is detected in durian seed gum) [40, 41].

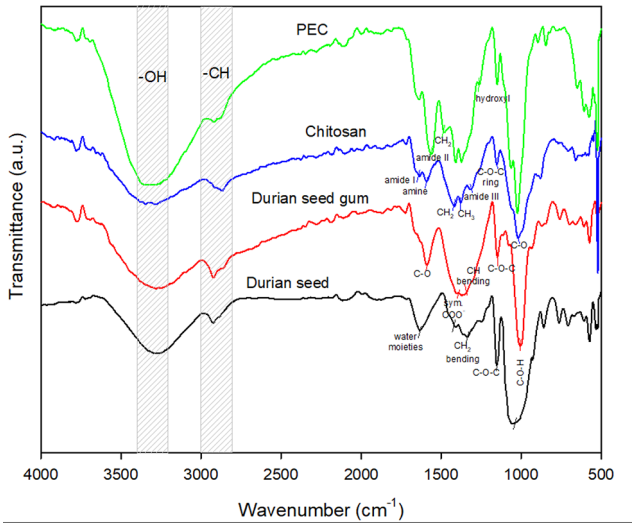


**Fig. 2** FTIR spectra of durian seed flour, DSG, chitosan, and PEC

Previous studies have shown that the yield of polysaccharides produced using the alkaline method is better than that produced using acid, water, or enzymatic extraction. Somboonpanyakul et al. (2006) extracted gum from malva nuts using sequential water, acid, and alkaline extraction; based on the results, the highest yield was around 20%, obtained through alkaline fractionation. Hot water and dilute acid extraction yielded ~ 1% and ~ 6%, respectively [35]. Another study extracted gum from flaxseed using different

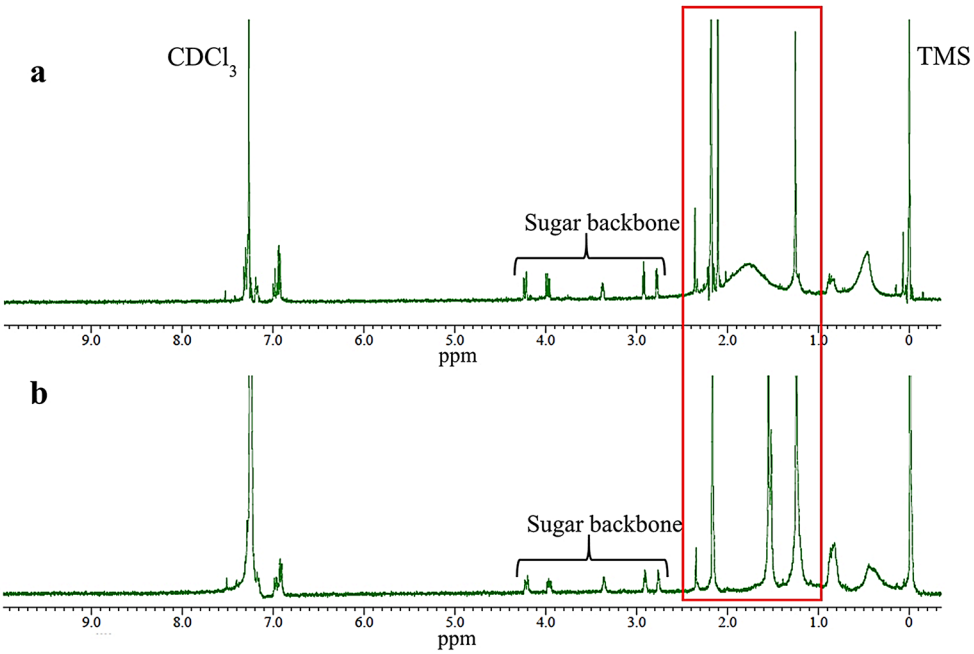


**Fig. 3** $^{1}$H NMR of (**a**) PEC and (**b**) DSG

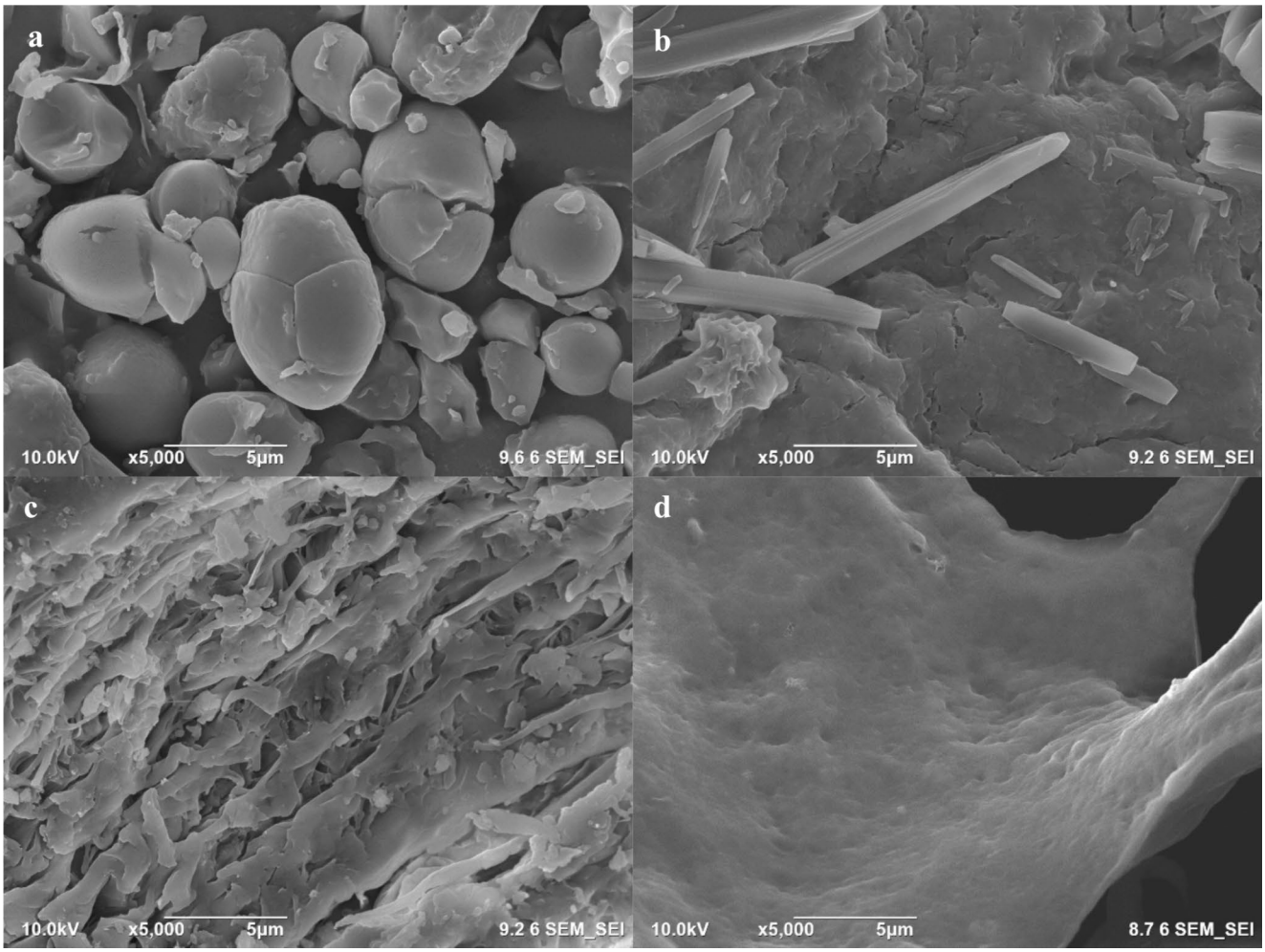


**Fig. 4** SEM images of **a**) durian seed flour, **b**) DSG, **c**) chitosan, and **d**) PEC DSG-chitosan

extraction methods; alkaline extraction generated the highest yield of flaxseed gum (13.7%), whereas enzymatic extraction yielded 4% and enzymatic ultrasonic extraction 2.85% [42]. Moreover, this study revealed a significantly high yield of gum using the alkaline method, which indicates the compatibility of alkaline hydrolysis with durian seeds.

The alkaline extraction method is well known for acquiring hemicellulose. Unlike cellulose, hemicellulose has a lower degree of polymerization (50–200) and is composed of many sugars (hexoses and pentoses). Combining ethanol precipitation with alkaline hydrolysis to obtain polysaccharides has also been widely used in many studies, especially for the raw materials from agricultural feedstocks. Bouaziz et al. (2016) examined the water-insoluble fraction of almond gum, which is the residue of almond gum after a series of treatments using hot water, alkaline, and ethanol precipitation; the precipitate is called almond gum hemicellulose [43]. The physical appearance of almond gum hemicellulose is very similar to that of durian seed gum (brown); the sugar profile is also high in glucose and has a low content of galactose and arabinose.

The alkali concentration also plays a significant role in the yield of mung bean polysaccharides; it has also been observed that the glucose content is higher than that of hot water extraction [44]. Alkali extraction can break the ester and hydrogen bonds between polysaccharides, enhancing the yield. Alkaline extraction is also used to extract corn fiber gum or hemicellulose B precipitates (with the addition of alcohol), which Kamboj and Rana investigated [6]. Hence, the term hemicellulose, polysaccharide, or gum is usually used to describe the extract from alkaline extraction.

### 3.3 Characterization of DSG and Chitosan complex coacervates

The spectra of durian seed, durian seed gum, chitosan, and PEC are depicted in Fig. 2, where all have similar transmittance around 3300 $cm^{-1}$ and 2900 $cm^{-1}$, corresponding to –OH and –CH stretching vibrations, respectively. Based

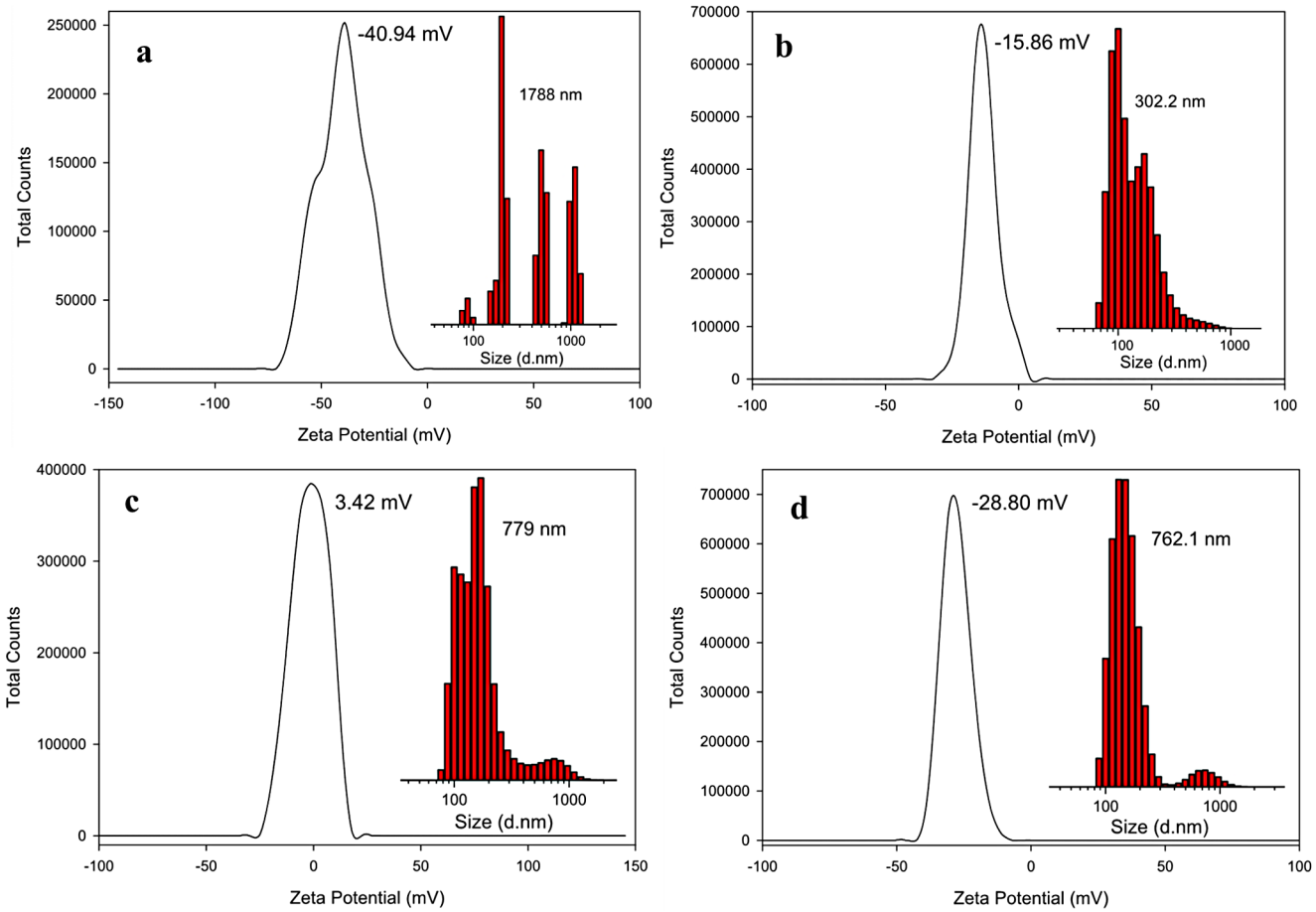


**Fig. 5** Zeta potential and particle size of (**a**) DSG in sodium hydroxide solution, (**b**) chitosan in acetic acid solution, (**c**) PEC in SGF, and (**d**) PEC in SIF

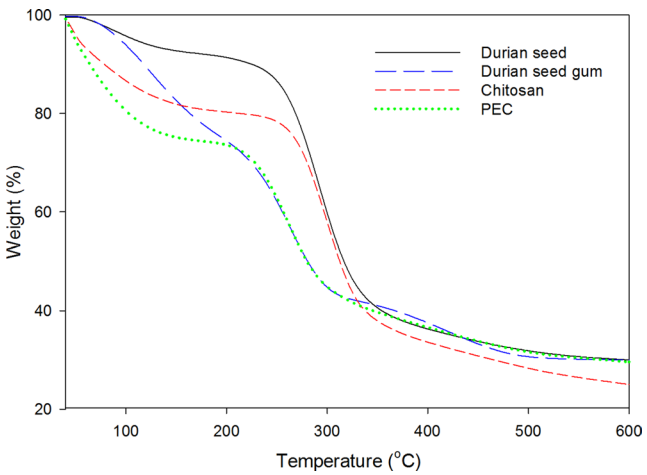


**Fig. 6** TGA of durian seeds, DSG, chitosan, and PEC

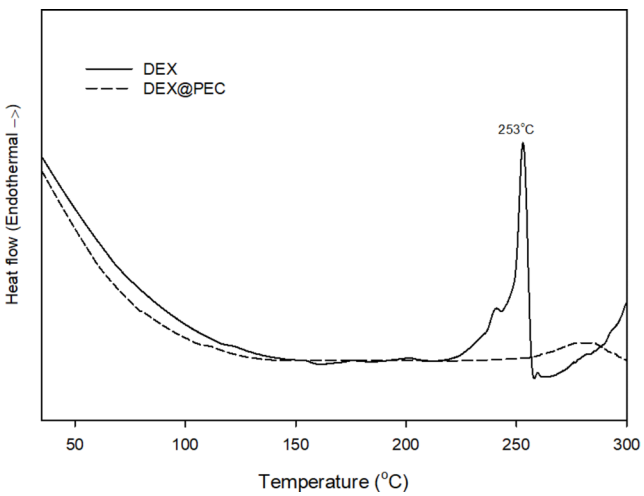


**Fig. 7** DSC thermograms of pure dexamethasone and DEX@PEC

on the FTIR spectra of durian seed and durian seed gum, the wavenumbers of durian gum shifted slightly compared to those of durian seed due to other compounds in the durian seed, such as amino acids and fatty acids. The peaks of the extracted gum at 1590 $cm^{-1}$ and 1370 $cm^{-1}$ indicate the asymmetric stretching of C-O and CH bending, respectively [21, 45]. Moreover, durian seed peaks at 1632 $cm^{-1}$, corresponding to adsorbed water moieties, and 1338 $cm^{-1}$ are attributed to $CH_2$ bending of carbohydrates [45, 46].

Several peaks of durian seed and durian gum are similar; for example, the spectra around 1405 $cm^{-1}$ correspond to the symmetrical vibrations of carboxylic groups (sym. The peak at 1150 $cm^{-1}$ corresponds to the C–O–C vibration band of glycosidic linkages, at 1000 $cm^{-1}$ corresponds to the C–O–H deformation band, and at 930 $cm^{-1}$ corresponds to the stretching vibrations of glycosidic bonds [47–50]. The region below 800 $cm^{-1}$ is known as the skeletal vibration region of carbohydrates [49]. The peak at 1634 cm-1 corresponds to the stretching vibrations of C = O in the amide I group, while the neighboring peak at 1589 $cm^{-1}$ corresponds to the primary amine [51]. The peaks at 1418 $cm^{-1}$ and 1378 $cm^{-1}$ represent the $CH_2$ bending group and $CH_3$ symmetrical deformation bands, respectively, and the spectral peak at 1318 $cm^{-1}$ is attributed to amide III groups [52]. More general characteristic peaks of chitosan are at wavenumbers 1152 $cm^{-1}$ and 1019 $cm^{-1,}$ corresponding to the C–O–C ring and C–O stretching, respectively [53]. The spectra of PEC indicate the combination of chitosan and durian seed gum at 1637 $cm^{-1}$ (amide I group), 1409 $cm^{-1}$ (carboxyl group), 1373 $cm^{-1}$ ($CH_2$ bending group), 1150 $cm^{-1}$ (C–O–C ring in polysaccharide), 1063 $cm^{-1}$ and 1023 $cm^{-1}$ (C-O stretching). The new peak at 1558 $cm^{-1}$ in the PEC spectrum was attributed to amide II (N–H bending), while the peak at 1480 $cm^{-1}$ was attributed to $CH_2$ bending of galacturonic acid due to the interaction between chitosan and DSG, and the peak at 1262 $cm^{-1}$ was attributed to the hydroxyl group of chitosan [52, 54, 55]. These peaks indicate the ionic interaction between chitosan and DSG to form PEC.

The chemical shift of PEC occurred in the range of 1.0 to 2.5 ppm; one of these peaks corresponded to the amine group of chitosan. Note that the peak in DSG (see Fig. 3) at 1.5 ppm disappeared in the PEC, and the broad peak showed at ~ 2 ppm. This peak marked the successful addition of chitosan into the PEC network. For reference, D-galactose was employed as a sugar model (Figure S2). D-galactose exhibited chemical shifts similar to DSG, indicating the presence of sugar peaks (~ 3-5.1 ppm). Similar peaks were also shown in the PEC spectra, signifying the sugar backbone.

The morphological structure of each material is depicted in Fig. 4. Durian seed flour has a globular structure, indicating complex polysaccharides, fatty acid, and protein contents in durian seeds. After alkaline extraction, the DSG consists of a more planar surface and sticks, as shown in Fig. 4(b). The image of chitosan shows a stacked terrain with pores, as shown in Fig. 4(c). PEC has a smoother surface than chitosan and DSG, and it is also observed that chitosan is fully covered by DSG, as shown in Fig. 3(d). PEC has a sponge-like structure, which was confirmed in the swelling assay.

The surface charge and particle size of DSG and chitosan are shown in Fig. 5(a) and (b). Compared with chitosan, DSG has a more negative charge due to the carboxyl group in its backbone structure. The particle size varied for DSG, with an average size of 1788 nm, while chitosan had an average particle size of 302.2 nm. A positive PEC value is expected in SGF because the outside of PEC is chitosan, which is protonated at low pH because of the amine group with a pKa value of ~ 6.5. Furthermore, PEC in SIF has a negative charge (-28.80 mV) caused by the interaction of sugar monomers and amine groups in the phosphate buffer solution. The sizes of the PEC particles in SGF and SIF were 779 nm and 762.1 nm, respectively. However, the particle distribution is even for PEC in SIF more than in SGF, which can be observed in Fig. 4(c) and (d). These results indicate that pH significantly influences the behavior of PEC in solution.

### 3.4 TGA and DSC analysis

Based on the thermal analysis, which can be seen in Fig. 6, there are three stages of degradation. The degradation temperatures of durian seeds and chitosan were similar in the 1st degradation stage, at approximately 230 °C. Durian seed and chitosan resulted in 10% and 20% weight loss, respectively. DSG and PEC have similar degradation temperatures at 200 °C, with 25% weight loss, which is slightly more significant than the weight loss of durian seed and chitosan. The second stage of degradation occurs until the temperature reaches 330 °C. The weight loss for durian seed was 50%, and that for chitosan was 37%. DSG and PEC have similar % weight loss, around 33%, indicating that PEC's thermal stability is more similar to DSG than chitosan.

The thermal properties of the drug and PEC were observed by DSC, as depicted in Fig. 7. The interaction between DEX and PEC was also investigated to understand the drug characteristics of the coacervates better. The thermogram of pure DEX showed a high-intensity endothermic peak at 253 °C ($\Delta H = 136.13$ J/g), indicating the melting peak of DEX. The melting temperature of dexamethasone is around 260 °C, as reported in previous studies [56, 57]. The DEX@PEC thermogram does not show a peak, which indicates that the encapsulated drug is in the coacervate of the DSG and chitosan complex. This phenomenon is also known as amorphization, a method commonly used in the pharmaceutical industry, especially for developing poorly water-soluble active pharmaceutical ingredients (APIs) [58]. The disappearance of the crystalline peak of dexamethasone is affected by the formulation of PEC, which has a large particle size of around 760–780 nm, and it can be concluded that dexamethasone is present in the dissolved state in the complex coacervate of DSG and chitosan [59].

### 3.5 Swelling assay

The behavior of PEC at SGF and SIF was investigated to understand the condition of coacervates in aqueous solution. The swelling of the material is strongly correlated with the ability or mechanism of the carrier to release the drug in SGF and SIF. Figure 8 shows that PEC has opposite swelling effects on SGF and SIF. The PEC in SGF constantly swelled up to 350% and decreased over time, while it continuously swelled in SIF. This result indicates that PEC is pH-responsive and suitable as a controlled drug delivery carrier, especially for colon-targeted drug delivery. PEC exhibited a sudden swelling of around 350% in the first hour and gradually decreased to 150% after 48 h of immersion in SGF. Chitosan is protonated at lower pH (pH < 4), and the amine groups are ionized to ammonium ions ($NH_3^+$), which causes rapid swelling of PEC under acidic conditions [60]. In addition, chitosan is highly soluble under acidic conditions, which could induce the erosion of PEC [61]. This is the main reason for the sudden decrease in the swelling degree of PEC at pH 2.0. The MW of chitosan also influenced the erosion of the matrix PEC, and low-MW chitosan eroded faster than did high-MW chitosan (200 kDa). Low-MW chitosan shows a greater percentage of erosion in acidic than in neutral pH media [62]. Moreover, the DSG in SGF is stable; there are no large differences in the degree of swelling after more than 10 h of immersion since the carboxyl groups in DSG are in the form of COOH.

Meanwhile, in pH 7.4, the swelling of PEC constantly increased throughout the immersion in SIF. During the first hour in SIF, the swelling degree of PEC is almost two times that in SGF. In a buffer solution, the carboxyl group of DSG is dissociated into $–COO^-$ ions [63, 64]. The intermolecular forces between the amine group and carboxyl anion weaken and allow the water to slowly penetrate from the surface of the PEC toward the core, which causes the swelling to increase exponentially for up to 10 h and expand to 550% at 48 h [65].

Several reports have shown that a lower gum ratio leads to more swelling. A lower gum concentration makes the coacervate complex more porous and increases PEC swelling [66]. A low xanthan gum solution (0.5% (w/v)) has a 50% greater degree of swelling than a 0.7% (w/v) xanthan solution, with moderate concentrations of chitosan (0.7% and 1.0% (w/v)) [67]. Excess chitosan in the PEC of gum kondagogu–chitosan (gum/chitosan = 1:3) also shows maximal swelling compared with that of gum (5:1 and 3:1) at pH 1.2 and pH 6.8 [68]. The swelling behavior of the hydrogel mixture of guar gum and chitosan is satisfactory for blends of guar gum and chitosan at 20% and 60% [69]. A study of the dynamic swelling behavior of the hydrogel xanthan–chitosan also revealed a more prolonged equilibrium

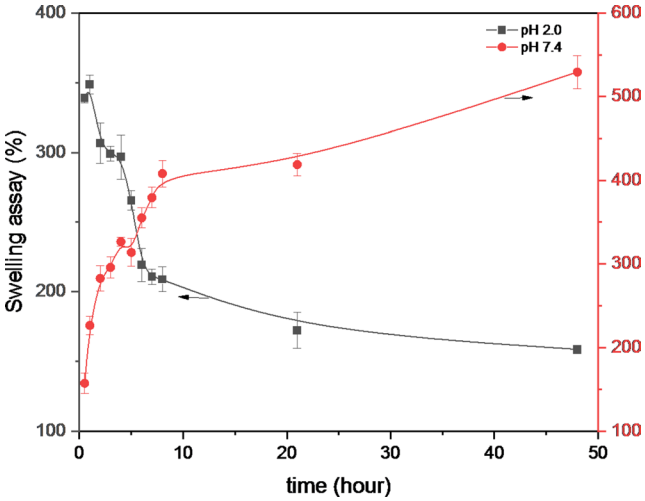


**Fig. 8** Swelling degree of PEC durian seed gum–chitosan at pH 2.0 (SGF) and pH 7.4 (SIF)

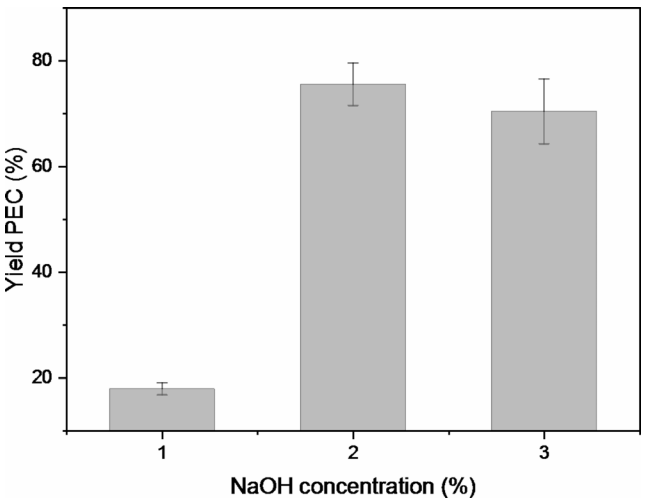


**Fig. 9** The effect of NaOH concentration on the formation of PECs

swelling time with 0.7% (w/v) xanthan gum than with 1% (w/v) xanthan gum and the required time to reach equilibrium swelling ratio was 6 h and 2 h, respectively [70]. This study prepared PECs with a smaller ratio of gum to chitosan (DSG/chitosan = 1:4) for controlled drug release in simulated gastric and intestinal fluid.

### 3.6 Drug loading and release

The NaOH solution concentration affected the yield of PEC, as shown in Fig. 9. By increasing the NaOH concentration, it can be seen that the PEC synthesized was best at 2% NaOH concentration, which was around 75.53%. The influence of NaOH on the formation of PECs is driven by the coagulation of chitosan under alkaline conditions. First, chitosan is solubilized in acetic acid, which causes the protonation of the amino groups of glucosamine. Afterward, this protonated

amine reacts with the hydroxyl ions of NaOH. The kinetics of chitosan coagulation in alkaline media (NaOH or urea) have been investigated by several researchers [71, 72]. The coagulation of chitosan is driven by the concentration of NaOH, which occurs instantaneously and follows Fick's second law of diffusion. This parameter is further used for dexamethasone entrapment in the PEC. Two different concentrations of dexamethasone (0.5 mg/mL and 1 mg/mL) were used to observe the loading and entrapment efficiency of the drug in PECs. The results are summarized in Table 3, which shows that the entrapment of the drug was supported by the bulk concentration of the drug under the initial conditions. The entrapment efficiency was stable for both concentrations; more than 90% of the drug was encapsulated in the gum and chitosan complex. The loading content of the drug is around 2 and 4 mg/g PEC for initial DEX concentrations of 0.5 and 1 mg/mL, respectively.

The release profile of the drug is depicted in Fig. 10, which shows a major difference in the cumulative release between the free and loaded drugs. The release profile is plotted against three models; the equations are described below.

$$R_t = \frac{R_m\, t^{\alpha}}{(t_{0.5} + t^{\alpha})} \tag{6}$$

$$R_t = k_P t^n \tag{7}$$

$$R_t = k_H t^{0.5} \tag{8}$$

Equations (6–8) represent the model fitting of Sigmoidal Hill, Korsmeyer–Peppas, and Higuchi, respectively [73, 74]. where $R_t$ is the cumulative release of the drug at a certain time (%), $_t$ is the time (h), $R_m$ is the maximum release of the drug (%), $t_{0.5}$ is the time to reach half of the maximum cumulative release (h), $_\alpha$ is a characteristic sigmoidal factor that is specific for a certain drug and carrier system, $k_P$ is the Korsmeyer–Peppas constant, $_n$ is the release exponent, and $k_H$ is the Higuchi constant.

**Table 3** The loading content and entrapment efficiency of DEX

| The concentration of DEX (mg/mL) | Entrapment efficiency (%) | Loading content (mg/g) |
|---|---|---|
| 0.5 | 93.39 ± 2.32 | 1.90 ± 0.12 |
| 1 | 95.79 ± 1.85 | 3.90 ± 0.06 |

**Table 4** Fitting parameters for drug release

| Solution | Data | Higuchi | Korsmeyer Peppas | Sigmoidal Hill |
|---|---|---|---|---|
| SGF | Free DEX | $k_H$ = 16.36 $R^2$ = 0.92 | $k_p$ = 12.31 $n$ = 0.79 $R^2$ = 0.98 | $R_m$ = 45.66% $t_{0.5}$ = 1.91 h α = 1.61 $R^2$ = 0.99 |
| | DEX@PEC | $k_H$ = 10.10 $R^2$ = 0.85 | $k_p$ = 5.99 $n$ = 1.02 $R^2$ = 0.98 | $R_m$ = 38.39% $t_{0.5}$ = 2.98 h α = 1.68 $R^2$ = 0.99 |
| SIF | Free DEX | $k_H$ = 18.14 $R^2$ = 0.92 | $k_p$ = 13.46 $n$ = 0.65 $R^2$ = 0.98 | $R_m$ = 94.24% $t_{0.5}$ = 6.44 h α = 1.21 $R^2$ = 0.99 |
| | DEX@PEC | $k_H$ = 10.85 $R^2$ = 0.91 | $k_p$ = 6.07 $n$ = 0.78 $R^2$ = 0.98 | $R_m$ = 52.70% $t_{0.5}$ = 5.93 h α = 1.59 $R^2$ = 0.99 |

All models show a high $R^2$ value above 0.90 for the fitting results of Korsmeyer Peppas and Hill (see Table 4), corresponding to a satisfactory experimental data fit. However, based on the plotting result in Fig. 10, the best-fitting results are obtained using the sigmoidal Hill equation in both SGF

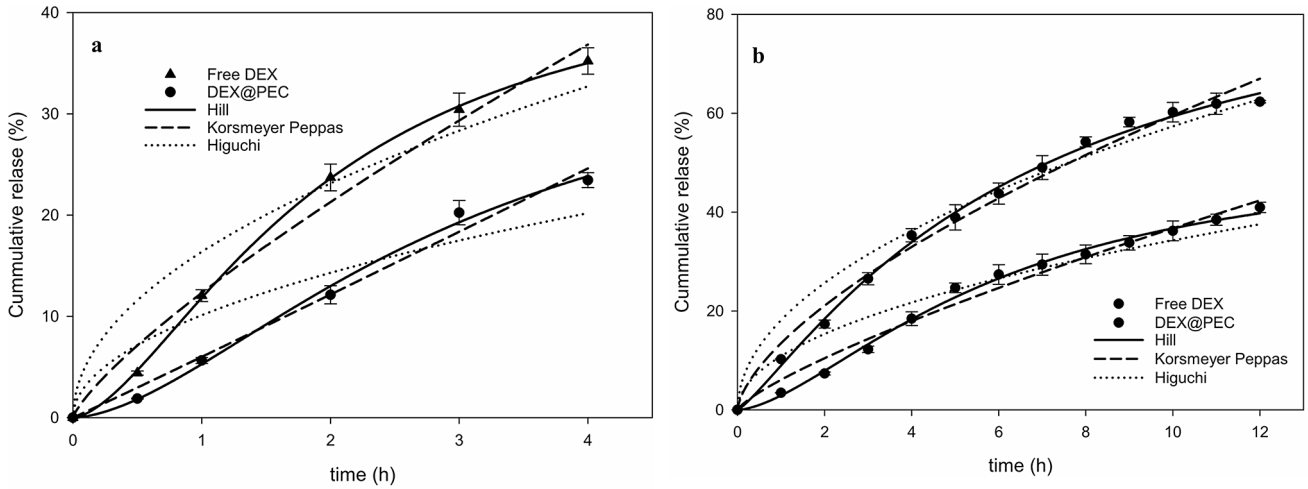


**Fig. 10** The release profile of the free drug and loaded drug DEX@PEC in (**a**) SGF and (**b**) SIF

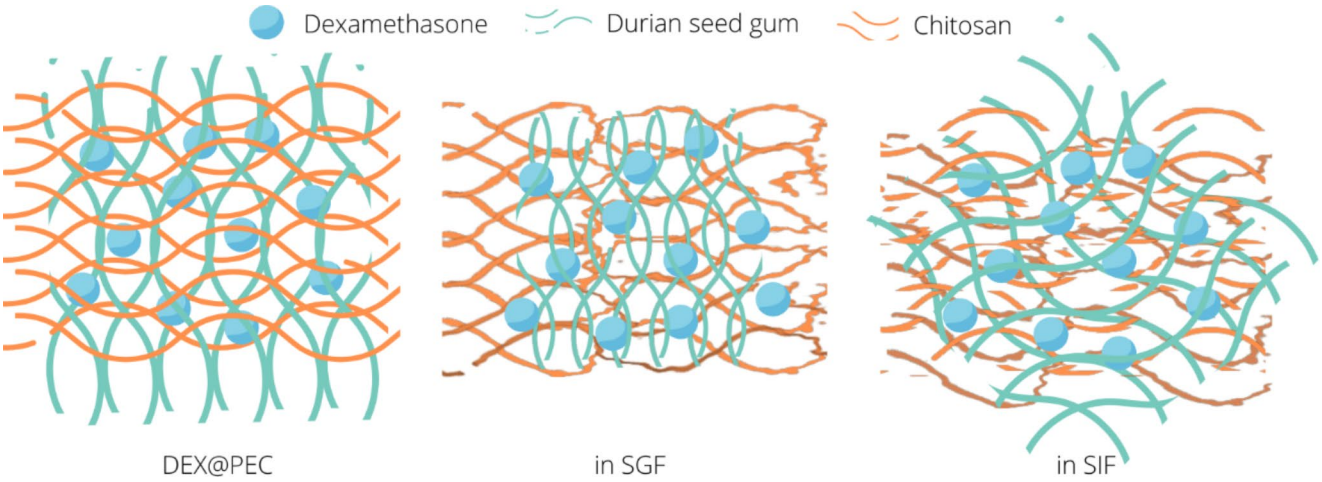


**Fig. 11** Mechanism of drug release from DEX@PEC

and SIF. The Hill equation is categorized as an empirical sigmoidal model with three parameters, a generalization of the Michaelis-Menten equation [75]. Hill first introduced it to describe oxygen binding in hemoglobin in 1910 [76]. The value of α influences the slope of the curve; where α is greater than 1 the curve has a steeper slope in the central portion [77]. The Hill equation is useful for describing the drug concentration-effect relationship in pharmacokinetic studies [78].

The values of the parameters fitted using Eq. (6) are listed in Table 4; the values of $R_m$ are 94% and 52% for free DEX and DEX@PEC in SIF, respectively. This parameter indicates that the release of drugs in the system will eventually reach the maximum release percentage according to the $R_m$ value, as shown in Table 4. The time required to reach 50% of the maximum release ($R_m$) is described by the parameter $t_{0.5}$. This parameter's value for free DEX was around 6.4 h, and that for DEX@PEC was almost 6 h. Note that Higuchi failed to fit the release of both data points in SGF and SIF; this behavior implies that DEX's release did not follow Fickian diffusion. The fitting result of Kosmeyer-Peppas further confirmed that both release profiles follow a non-Fickian model with a value of $_n$ between 0.5 and 1.0 in SIF. Observing the fitting of the experimental shows the importance of α, which signifies Hill's compatibility in both pH conditions. The value of α plays an important role in Hill equation to have the flexibility to adjust the fitting results.

The purpose of PEC is to form a network between cationic chitosan and anionic polysaccharide gum, and the interaction of this oppositely charged material results in complex formation. From the results of the release of DEX@PEC, a slower cumulative release percentage was achieved at pH 7.4 than at pH 2.0. This indicates that the mechanism of DEX@PEC drug release was driven by the swelling action of PEC, which was induced by changing the pH (illustrated in Fig. 11). As mentioned in the swelling assay, PEC undergoes sudden swelling, followed by a decrease in the swelling degree, indicating the erosion of chitosan in the network of PEC. A study of the swelling kinetics of chitosan showed that at pH 6.8, Fickian diffusion occurred, while at pH 1.2, the diffusion was close to zero due to the very loose gel structure of chitosan at low pH, which induced gel erosion [79, 80]. This phenomenon causes a faster cumulative release in SGF, with a cumulative release of 10% within 2 h. The fitted model at pH 2.0 also indicated that Higuchi and Korsmeyer-Peppas could not fully fit the release profile like Fickian diffusion.

## 4 Conclusion

The gum extraction from durian seeds was successful, with a yield of 58%, an extraction time of 20 min, a temperature of 60 °C, a water-to-solid ratio of 50:1, and a pH of 13. The extracted durian seed gum contained sugar monomers such as glucose, galactose, and arabinose, similar to previous studies. Durian seed gum and chitosan have promising applications in controlled drug delivery; the predicted maximum cumulative release is around 51%, with an extended release time of more than 10 h. The empirical sigmoidal Hill equation is flexible enough to fit the overall release data in this study. DEX@PEC has a mechanism of polymer swelling due to pH changes; these data were confirmed through a swelling assay. The interaction of the opposite charge between the carboxyl ions in gum and the amine ions in chitosan formed a complex network aggregate since the ratio of chitosan to gum was 4 to 1.

**Supplementary Information** The online version contains supplementary material available at https://doi.org/10.1007/s42247-024-00843-6.

**Acknowledgements** This work was supported by the Ministry of Education, Culture, Research, and Technology of the Republic of Indonesia through a Fundamental research grant and a competitive research funding from Universitas Katolik Widya Mandala Surabaya.

**Author contributions** JN Putro: Conceptualization, Formal analysis, Writing – Original draft, Funding acquisition. HF Tulus: Investigation, Software. CJ Wijaya: Project administration. D Mangindaan: Data curation. W Irawaty: Validation. C Gunarto: Visualization. N Puspitasari: Visualization. AE Angkawijaya: Resources. A Rahmawati: Formal analysis, Investigation. O Shinomura: Resources. S Ismadji: Supervision, Resources, Writing – Review & Editing.

**Data availability** The data that support the findings of this study are available from the corresponding author (Putro JN), upon request.

## Declarations

**Competing interest** The authors declare that they have no known competing financial interests or personal relationships that could have appeared to influence the work reported in this paper.

## References

1. S. Chadha, Recent advances in nano-encapsulation technologies for controlled release of biostimulants and antimicrobial agents, in *Adv. Nano-Fertilizers Nano-Pesticides Agric*, ed. by S. Jogaiah, H.B. Singh, L.F. Fraceto, R. de Lima (Elsevier, 2021), pp. 29–55. https://doi.org/10.1016/B978-0-12-820092-6.00002-1
2. S. Jana, S. Maiti, S. Jana, Stimuli-responsive guar gum composites for colon-specific drug delivery. Elsevier Ltd. (2017). https://doi.org/10.1016/B978-0-08-101914-6.00003-X
3. M. Bahramparvar, H.D. Goff, Basil seed gum as a novel stabilizer for structure formation and reduction of ice recrystallization in ice cream. Dairy. Sci. Technol. **93**, 273–285 (2013). https://doi.org/10.1007/s13594-013-0122-9
4. S. Gupta, P.S. Variyar, *Guar Gum: A Versatile Polymer for the Food Industry* (Elsevier Inc., 2018). https://doi.org/10.1016/B978-0-12-811449-0.00012-8
5. M. Cornelia, T. Siratantri, R. Prawita, The utilization of Extract Durian (Durio zibethinus L.) seed gum as an Emulsifier in Vegan Mayonnaise. Procedia Food Sci. **3**, 1–18 (2015). https://doi.org/10.1016/j.profoo.2015.01.001
6. S.-C. Wu, Y.-S. Shyu, Y.-W. Tseng, W.-C. Sung, The effect of tamarind seed gum on the qualities of Gluten-Free cakes. Processes. **8**, 318 (2020). https://doi.org/10.3390/pr8030318
7. Production of Fruits, 2020, Stat. Indones. (2021). https://www.bps.go.id/indicator/55/62/1/produksi-tanaman-buah-buahan.html (accessed November 12, 2021)
8. B.T. Amid, H. Mirhosseini, E. Activity, Particle uniformity and Rheological properties of a natural polysaccharide-protein Biopolymer from Durian seed. Food Biophys. **7**, 317–328 (2012). https://doi.org/10.1007/s11483-012-9270-3
9. B.T. Amid, H. Mirhosseini, S. Kostadinović, Chemical composition and molecular structure of polysaccharide-protein biopolymer from Durio zibethinus seed: extraction and purification process. Chem. Cent. J. **6**, 1–14 (2012). https://doi.org/10.1186/1752-153X-6-117
10. P. Varichanan, S. Shompoosang, S. Dueramae, Potential Prebiotic properties of Crude Polysaccharide Extract from Durian (Durio zibethinus Murr.) Seed flour. Trends Sci. **20** (2023). https://doi.org/10.48048/tis.2023.6770
11. J.J.L. Lee, G. Zhao, J. Kim, C. Castillo-Zacarias, M.T. Ramirez-Arriaga, R. Parra-Saldivar, W.N. Chen, Dual use of a Biopolymer from Durian (Durio zibethinus) seed as a nutrient source and Stabilizer for Spray Dried Lactobacillus Plantarum, Front. Sustain. Food Syst. **2**, 1–9 (2018). https://doi.org/10.3389/fsufs.2018.00053
12. P. Ningsih, I. Said, B. Hamzah, I. Made Tangkas, S. Rahmawati, I.K. Bissin, The potential of Durian seed flour as an alternative source of Carbohydrate for Diabetes Mellitus sufferers. Eur. J. Mol. Clin. Med. (2021)
13. V.S. Meka, M.K.G. Sing, M.R. Pichika, S.R. Nali, V.R.M. Kolapalli, P. Kesharwani, A comprehensive review on polyelectrolyte complexes. Drug Discov Today. **22**, 1697–1706 (2017). https://doi.org/10.1016/j.drudis.2017.06.008
14. L.R. de Sena Miranda, C.C. do, N.D. Cardoso, A.R. Almeida, M. do, S.M.A. do Nascimento, F.A.S.D. Pinheiro, S.A.B. de Moura, J.P.M. de Lima, Á.A.N. de Lima, E.G. Barbosa, W. de Morais, C. Camillo, Development, characterization, and in-vivo evaluation of a novel chitosan: Guar gum particulate system for colonic release of triamcinolone, J. Drug Deliv. Sci. Technol. 96 (2024). https://doi.org/10.1016/j.jddst.2024.105726
15. C. Roy, A. Gandhi, S. Manna, S. Jana, Fabrication and evaluation of carboxymethyl guar gum-chitosan interpenetrating polymer network (IPN) nanoparticles for controlled drug delivery. Med. Nov Technol. Devices. **22**, 100300 (2024). https://doi.org/10.1016/j.medntd.2024.100300
16. M. Minkal, D.C. Ahuja, Bhatt, Polyelectrolyte complex of carboxymethyl gum katira-chitosan: Preparation and characterization. Int. J. Biol. Macromol. **106**, 1184–1191 (2018). https://doi.org/10.1016/j.ijbiomac.2017.08.128
17. M. Minkal, D.C. Ahuja, Bhatt, Carboxymethyl gum katira: synthesis, characterization and evaluation for nanoparticulate drug delivery. RSC Adv. **5**, 82363–82373 (2015). https://doi.org/10.1039/c5ra11702j
18. R. Samanta, S. Nayak, B. Das, A.K. Nayak, Chitosan-carboxymethyl tamarind gum in situ polyelectrolyte complex-based floating capsules of ofloxacin: in vitro-in vivo studies. Int. J. Biol. Macromol. **253**, 127507 (2023). https://doi.org/10.1016/j.ijbiomac.2023.127507
19. J. Potaś, R.A. Wach, B. Rokita, M. Wróblewska, K. Winnicka, Evaluation of the impact of tragacanth/xanthan gum interpolymer complexation with chitosan on pharmaceutical performance of gels with secnidazole as potential periodontal treatment. Eur. J. Pharm. Sci. 192 (2024). https://doi.org/10.1016/j.ejps.2023.106657
20. H.S. Mahajan, P.P. Patil, In situ cross linked Chitosan-Gellan Gum Polyelectrolyte Complex based nanogels containing curcumin for delivery to Cancer cells. Indian J. Pharm. Educ. Res. **51**, s40–s45 (2017). https://doi.org/10.5530/ijper.51.2s.48
21. A. Ćirić, Đ. Medarević, B. Čalija, V. Dobričić, M. Mitrić, L. Djekic, Study of chitosan/xanthan gum polyelectrolyte complexes formation, solid state and influence on ibuprofen release kinetics. Int. J. Biol. Macromol. **148**, 942–955 (2020). https://doi.org/10.1016/j.ijbiomac.2020.01.138
22. P.K. Kathle, N. Gautam, K. Kesavan, Tamoxifen citrate loaded chitosan-gellan nanocapsules for breast cancer therapy: development, characterisation and in-vitro cell viability study. J. Microencapsul. **35**, 292–300 (2018). https://doi.org/10.1080/02652048.2018.1477844
23. S. Noreen, F. Pervaiz, A. Ashames, M. Buabeid, K. Fahelelbom, H. Shoukat, I. Maqbool, G. Murtaza, Optimization of Novel Naproxen-Loaded Chitosan/Carrageenan Nanocarrier-based gel for topical delivery: Ex vivo, histopathological, and in vivo evaluation, Pharmaceuticals. 14 (2021). https://doi.org/10.3390/ph14060557
24. L. Li, L. Wang, J. Li, S. Jiang, Y. Wang, X. Zhang, J. Ding, T. Yu, S. Mao, Insights into the mechanisms of chitosan–anionic

polymers-based matrix tablets for extended drug release. Int. J. Pharm. **476**, 253–265 (2014). https://doi.org/10.1016/j.ijpharm.2014.09.057
25. S. Noreen, I. Maqbool, A. Madni, Therapeutic potential, risks, and future projection during COVID-19 pandemic. Eur. J. Pharmacol. **894**, 173854 (2021). https://doi.org/10.1016/j.ejphar.2021.173854
26. M.H. Ahmed, A. Hassan, Dexamethasone for the treatment of Coronavirus Disease (COVID-19): a review, SN Compr. Clin. Med. **2**, 2637–2646 (2020). https://doi.org/10.1007/s42399-020-00610-8
27. S. Jain, M. Datta, Oral extended release of dexamethasone: Montmorillonite – PLGA nanocomposites as a delivery vehicle. Appl. Clay Sci. **104**, 182–188 (2015). https://doi.org/10.1016/j.clay.2014.11.028
28. J. Long, A.V. Nand, C. Bunt, A. Seyfoddin, Controlled release of dexamethasone from poly(vinyl alcohol) hydrogel. Pharm. Dev. Technol. **24**, 839–848 (2019). https://doi.org/10.1080/10837450.2019.1602632
29. X. Li, L. Xu, H. Nie, L. Lei, Dexamethasone-loaded β-cyclodextrin for osteogenic induction of mesenchymal stem/progenitor cells and bone regeneration. J. Biomed. Mater. Res. Part. A **109**, 1125–1135 (2021). https://doi.org/10.1002/jbm.a.37104
30. K. Dong, Y. Dong, C. You, W. Xu, X. Huang, Y. Yan, L. Zhang, K. Wang, J. Xing, Assessment of the drug loading, in vitro and in vivo release behavior of novel pH-sensitive hydrogel. Drug Deliv. **23**, 174–184 (2016). https://doi.org/10.3109/10717544.2014.908329
31. L. Lei, U. Larry, Controlled release of dexamethasone from in situ forming nanofiber - nanoparticle hybrid hydrogel. Front. Bioeng. Biotechnol. **4** (2016). https://doi.org/10.3389/conf.FBIOE.2016.01.01786
32. Y.P. Timilsena, T.O. Akanbi, N. Khalid, B. Adhikari, C.J. Barrow, International Journal of Biological Macromolecules Complex coacervation: principles, mechanisms and applications in microencapsulation. Int. J. Biol. Macromol. **121**, 1276–1286 (2019). https://doi.org/10.1016/j.ijbiomac.2018.10.144
33. Y. Luo, Q. Wang, Y. Zhang, Biopolymer-Based Nanotechnology Approaches To Deliver Bioactive Compounds for Food Applications: A Perspective on the Past, Present, and, Future, J. Agric. Food Chem. 68 (2020) 12993–13000. https://doi.org/10.1021/acs.jafc.0c00277
34. H. Karazhiyan, S.M.A. Razavi, G.O. Phillips, Extraction optimization of a hydrocolloid extract from cress seed (Lepidium sativum) using response surface methodology. Food Hydrocoll. **25**, 915–920 (2011). https://doi.org/10.1016/j.foodhyd.2010.08.022
35. P. Somboonpanyakul, Q. Wang, W. Cui, S. Barbut, P. Jantawat, Malva nut gum. (part I): extraction and physicochemical characterization. Carbohydr. Polym. **64**, 247–253 (2006). https://doi.org/10.1016/j.carbpol.2005.11.034
36. M. Fathi, Z. Emam-Djomeh, A. Sadeghi-Varkani, Extraction, characterization and rheological study of the purified polysaccharide from Lallemantia Ibrica seeds. Int. J. Biol. Macromol. **120**, 1265–1274 (2018). https://doi.org/10.1016/j.ijbiomac.2018.08.159
37. L.R. Van Loon, M.A. Glaus, *Experimental and Theoretical Studies on Alkaline Degradation of Cellulose and its Impact on the Sorption of Radionuclides* (Paul Scherrer Institut, 1998)
38. H. Karazhiyan, S.M.A. Razavi, G.O. Phillips, Food hydrocolloids extraction optimization of a hydrocolloid extract from cress seed (Lepidium sativum) using response surface methodology. Food Hydrocoll. **25**, 915–920 (2011). https://doi.org/10.1016/j.foodhyd.2010.08.022
39. B.T. Amid, H. Mirhosseini, Optimisation of aqueous extraction of gum from durian (Durio zibethinus) seed: a potential, low cost source of hydrocolloid. Food Chem. **132**, 1258–1268 (2012). https://doi.org/10.1016/j.foodchem.2011.11.099
40. A. Koocheki, A.R. Taherian, S.M.A. Razavi, A. Bostan, Response surface methodology for optimization of extraction yield, viscosity, hue and emulsion stability of mucilage extracted from Lepidium perfoliatum seeds. Food Hydrocoll. **23**, 2369–2379 (2009). https://doi.org/10.1016/j.foodhyd.2009.06.014
41. A.M. Amin, A.S. Ahmad, Y.Y. Yin, N. Yahya, N. Ibrahim, Extraction, purification and characterization of durian (Durio zibethinus) seed gum. Food Hydrocoll. **21**, 273–279 (2007). https://doi.org/10.1016/j.foodhyd.2006.04.004
42. M. Moczkowska, S. Karp, Y. Niu, M.A. Kurek, Enzymatic, enzymatic-ultrasonic and alkaline extraction of soluble dietary fibre from flaxseed – a physicochemical approach. Food Hydrocoll. **90**, 105–112 (2019). https://doi.org/10.1016/j.foodhyd.2018.12.018
43. F. Bouaziz, M. Koubaa, K. Ben Jeddou, F. Kallel, C. Boisset Helbert, A. Khelfa, R. Ellouz Ghorbel, Ellouz Chaabouni, Water-soluble polysaccharides and hemicelluloses from almond gum: functional and prebiotic properties. Int. J. Biol. Macromol. **93**, 359–368 (2016). https://doi.org/10.1016/j.ijbiomac.2016.08.032
44. S. Chen, L. Qin, L. Xie, Q. Yu, Y. Chen, T. Chen, H. Lu, J. Xie, Physicochemical characterization, rheological and antioxidant properties of three alkali-extracted polysaccharides from mung bean skin. Food Hydrocoll. **132**, 107867 (2022). https://doi.org/10.1016/j.foodhyd.2022.107867
45. P. Zhang, S.J. Dong, H.H. Ma, B.X. Zhang, Y.F. Wang, X.M. Hu, Fractionation of corn stover into cellulose, hemicellulose and lignin using a series of ionic liquids. Ind. Crops Prod. **76**, 688–696 (2015). https://doi.org/10.1016/j.indcrop.2015.07.037
46. X.F. Sun, F. Xu, R.C. Sun, Z.C. Geng, P. Fowler, M.S. Baird, Characteristics of degraded hemicellulosic polymers obtained from steam exploded wheat straw. Carbohydr. Polym. **60**, 15–26 (2005). https://doi.org/10.1016/j.carbpol.2004.11.012
47. S. Vasiliu, I. Bunia, S. Racovita, V. Neagu, Adsorption of cefotaxime sodium salt on polymer coated ion exchange resin microparticles: kinetics, equilibrium and thermodynamic studies. Carbohydr. Polym. **85**, 376–387 (2011). https://doi.org/10.1016/j.carbpol.2011.02.039
48. S. Pavlovic, P.R.G. Brandao, Adsorption of starch, amylose, amylopectin and glucose monomer and their effect on the flotation of hematite and quartz. Min. Eng. **16**, 1117–1122 (2003). https://doi.org/10.1016/j.mineng.2003.06.011
49. T. Hong, J.Y. Yin, S.P. Nie, M.Y. Xie, Applications of infrared spectroscopy in polysaccharide structural analysis: Progress, challenge and perspective. Food Chem. X. **12**, 100168 (2021). https://doi.org/10.1016/j.fochx.2021.100168
50. N.A. Nikonenko, D.K. Buslov, N.I. Sushko, R.G. Zhbankov, Spectroscopic manifestation of stretching vibrations of glycosidic linkage in polysaccharides. J. Mol. Struct. **752**, 20–24 (2005). https://doi.org/10.1016/j.molstruc.2005.05.015
51. I.K.D. Dimzon, T.P. Knepper, Degree of deacetylation of chitosan by infrared spectroscopy and partial least squares. Int. J. Biol. Macromol. **72**, 939–945 (2015). https://doi.org/10.1016/j.ijbiomac.2014.09.050
52. M.F. Queiroz, K.R.T. Melo, D.A. Sabry, G.L. Sassaki, H.A.O. Rocha, Does the use of Chitosan contribute to oxalate kidney stone formation? Mar. Drugs. **13**, 141–158 (2015). https://doi.org/10.3390/md13010141
53. G. Lawrie, I. Keen, B. Drew, A. Chandler-Temple, L. Rintoul, P. Fredericks, L. Grøndahl, Interactions between alginate and chitosan biopolymers characterized using FTIR and XPS. Biomacromolecules. **8**, 2533–2541 (2007). https://doi.org/10.1021/bm070014y
54. Y. Shao, L. Li, X. Gu, L. Wang, S. Mao, Evaluation of chitosan-anionic polymers based tablets for extended-release of highly water-soluble drugs. Asian J. Pharm. Sci. **10**, 24–30 (2015). https://doi.org/10.1016/j.ajps.2014.08.002

55. H. Munir, M. Shahid, F. Anjum, D. Mudgil, Structural, thermal and rheological characterization of modified Dalbergia sissoo gum-A medicinal gum. Int. J. Biol. Macromol. **84**, 236–245 (2016). https://doi.org/10.1016/j.ijbiomac.2015.12.001
56. N.M. Vacanti, H. Cheng, P.S. Hill, D.T. Guerreiro, T.T. Dang, M. Ma, R. Langer, N.S. Hwang, D.G. Anderson, Localized delivery of Dexamethasone from Electrospun fibers reduces the foreign body response. Biomacromolecules. **13**, 3031–3038 (2012). https://doi.org/10.1021/bm300520u
57. M. Alami-Milani, P. Zakeri-milani, H. Valizadeh, R. Salehi, M. Jelvehgari, Preparation and evaluation of PCL-PEG-PCL micelles as potential nanocarriers for ocular delivery of dexamethasone. Iran. J. Basic. Med. Sci. **21**, 153–164 (2018). https://doi.org/10.22038/IJBMS.2017.26590.6513
58. O. Jojart-Laczkovich, P. Szabo-Revesz, Amorphization of a crystalline active pharmaceutical ingredient and thermoanalytical measurements on this glassy form. J. Therm. Anal. Calorim. **102**, 243–247 (2010). https://doi.org/10.1007/s10973-009-0530-5
59. J. Panyam, D. Williams, A. Dash, D. Leslie-pelecky, V. Labhasetwar, Solid-state solubility influences encapsulation and release of hydrophobic drugs from PLGA/PLA Nanoparticles. J. Pharm. Sci. **93**, 1804–1814 (2004). https://doi.org/10.1002/jps.20094
60. H. Park, K. Park, D. Kim, Preparation and swelling behavior of chitosan-based superporous hydrogels for gastric retention application. J. Biomed. Mater. Res. Part. A **76A**, 144–150 (2005). https://doi.org/10.1002/jbm.a.30533
61. G. Pasparakis, N. Bouropoulos, Swelling studies and in vitro release of verapamil from calcium alginate and calcium alginate – chitosan beads. Int. J. Pharm. **323**, 34–42 (2006). https://doi.org/10.1016/j.ijpharm.2006.05.054
62. K. Huanbutta, K. Cheewatanakornkool, K. Terada, Impact of salt form and molecular weight of chitosan on swelling and drug release from chitosan matrix tablets. Carbohydr. Polym. **97**, 26–33 (2013). https://doi.org/10.1016/j.carbpol.2013.04.073
63. M. Gierszewska, J. Ostrowska-czubenko, E. Chrzanowska, pH-responsive chitosan / alginate polyelectrolyte complex membranes reinforced by tripolyphosphate. Eur. Polym. J. **101**, 282–290 (2018). https://doi.org/10.1016/j.eurpolymj.2018.02.031
64. K. De Yao, H. Tu, F. Cheng, J.W. Zhang, J. Liu, pH-Sensitivity of the swelling of a chitosan-pectin polyelectrolyte complex. Die Angew Makromol Chemie. **245**, 63–72 (1997)
65. X. Qu, A. Wirsen, A. Albertsson, Novel pH-sensitive chitosan hydrogels: swelling behavior and states of water. Polym. (Guildf). **41**, 4589–4598 (2000)
66. S. Rahman, A. Konwar, G. Majumdar, D. Chowdhury, Guar gum-chitosan composite film as excellent material for packaging application. Carbohydr. Polym. Technol. Appl. **2**, 100158 (2021). https://doi.org/10.1016/j.carpta.2021.100158
67. S. Argin-Soysal, P. Kofinas, Y.M. Lo, Effect of complexation conditions on xanthan – chitosan polyelectrolyte complex gels. Food Hydrocoll. **23**, 202–209 (2009). https://doi.org/10.1016/j.foodhyd.2007.12.011
68. V.G.M. Naidu, K. Madhusudhana, R.B. Sashidar, S. Ramakrishna, R.K. Khar, F.J. Ahmed, P.V. Diwan, Polyelectrolyte complexes of gum kondagogu and chitosan, as diclofenac carriers. Carbohydr. Polym. **76**, 464–471 (2009). https://doi.org/10.1016/j.carbpol.2008.11.010
69. D.N. Iqbal, S. Sha, S.M. Khan, S.M. Ibrahim, S.A. Abubshait, A. Nazir, M. Abbas, M. Iqbal, International Journal of Biological macromolecules Novel chitosan / guar gum / PVA hydrogel: Preparation, characterization and antimicrobial activity evaluation. Int. J. Biol. Ma. **164**, 499–509 (2020). https://doi.org/10.1016/j.ijbiomac.2020.07.139
70. S. Argin, P. Kofinas, Y.M. Lo, The cell release kinetics and the swelling behavior of physically crosslinked xanthan-chitosan hydrogels in simulated gastrointestinal conditions. Food Hydrocoll. **40**, 138–144 (2014). https://doi.org/10.1016/j.foodhyd.2014.02.018
71. Z. Qiao, Z. Wang, C. Zhang, S. Yuan, Y. Zhu, J. Wang, PVAm–PIP/PS composite membrane with high performance for $CO_2/N_2$ separation. AIChE J. **59**, 215–228 (2012). https://doi.org/10.1002/aic
72. A.A. Enache, L. David, J.P. Puaux, I. Banu, G. Bozga, Kinetics of chitosan coagulation from aqueous solutions. J. Appl. Polym. Sci. **135**, 1–12 (2018). https://doi.org/10.1002/app.46062
73. J. Siepmann, N.A. Peppas, Higuchi equation: derivation, applications, use and misuse. Int. J. Pharm. **418**, 6–12 (2011). https://doi.org/10.1016/j.ijpharm.2011.03.051
74. R.W. Korsmeyer, R. Gurny, E. Doelker, P. Buri, N.A. Peppas, Mechanisms of solute release from porous hydrophilic polymers. Int. J. Pharm. **15**, 25–35 (1983). https://doi.org/10.1016/0378-5173(83)90064-9
75. J. Heidel, J. Maloney, J. Aust Math. Soc. Ser. B-Applied Math. **41**, 83–92 (1999). https://doi.org/10.1017/s0334270000011048. When can sigmoidal data be fit to a Hill curve?
76. S.R. Gadagkar, G.B. Call, Computational tools for fitting the Hill equation to dose-response curves. J. Pharmacol. Toxicol. Methods. **71**, 68–76 (2015). https://doi.org/10.1016/j.vascn.2014.08.006
77. N.H.G. Holford, L.B. Sheiner, Understanding the dose-effect relationship. Clin. Pharmacokinet. **6**, 429–453 (1981). https://doi.org/10.2165/00003088-198106060-00002
78. H. Prinz, Hill coefficients, dose-response curves and allosteric mechanisms. J. Chem. Biol. **3**, 37–44 (2010). https://doi.org/10.1007/s12154-009-0029-3
79. K. Huanbutta, K. Terada, P. Sriamornsak, J. Nunthanid, European Journal of Pharmaceutics and Biopharmaceutics Advanced technologies for assessment of polymer swelling and erosion behaviors in pharmaceutical aspect. Eur. J. Pharm. Biopharm. **83**, 315–321 (2013). https://doi.org/10.1016/j.ejpb.2012.10.002
80. K. Huanbutta, P. Sriamornsak, S. Limmatvapirat, M. Luangtana-anan, European Journal of Pharmaceutics and Biopharmaceutics Swelling kinetics of spray-dried chitosan acetate assessed by magnetic resonance imaging and their relation to drug release kinetics of chitosan matrix tablets. Eur. J. Pharm. Biopharm. **77**, 320–326 (2011). https://doi.org/10.1016/j.ejpb.2010.11.019